All-fiber supercontinuum absorption spectroscopy for mid-infrared gas sensing

Rémi Bizot, Idris Tiliouine, Frédéric Désévédavy, Grégory Gadret, Clément Strutynski, Esteban Serrano, Pierre Mathey, Bertrand Kibler, Sébastien Février, Frédéric Smektala

▶ **To cite this version:**

Rémi Bizot, Idris Tiliouine, Frédéric Désévédavy, Grégory Gadret, Clément Strutynski, et al.. All-fiber supercontinuum absorption spectroscopy for mid-infrared gas sensing. APL Photonics, 2024, 9 (11), pp.111303. 10.1063/5.0230383 . hal-04840726

HAL Id: hal-04840726
https://hal.science/hal-04840726v1

Submitted on 16 Dec 2024

HAL is a multi-disciplinary open access archive for the deposit and dissemination of scientific research documents, whether they are published or not. The documents may come from teaching and research institutions in France or abroad, or from public or private research centers.

L'archive ouverte pluridisciplinaire **HAL**, est destinée au dépôt et à la diffusion de documents scientifiques de niveau recherche, publiés ou non, émanant des établissements d'enseignement et de recherche français ou étrangers, des laboratoires publics ou privés.

Distributed under a Creative Commons Attribution 4.0 International License

APL Photonics

LETTER | NOVEMBER 12 2024

All-fiber supercontinuum absorption spectroscopy for mid-infrared gas sensing

Special Collection: Mid-IR Photonics

Rémi Bizot ; Idris Tiliouine ; Frédéric Désévédavy ; Grégory Gadret ; Clément Strutynski ; Esteban Serrano ; Pierre Mathey; Bertrand Kibler ; Sébastien Février ; Frédéric Smektala

Check for updates

APL Photonics 9, 111303 (2024)
https://doi.org/10.1063/5.0230383

View Online
Export Citation

Articles You May Be Interested In

Supercontinuum Fourier transform spectrometry with balanced detection on a single photodiode

J. Chem. Phys. (August 2016)

Coherence property of mid-infrared supercontinuum generation in tapered chalcogenide fibers with different structures

Appl. Phys. Lett. (January 2016)

On-chip mid-infrared dispersive wave generation at targeted molecular absorption wavelengths

APL Photonics (August 2024)

16 December 2024 13:28:14

AMERICAN ELEMENTS
THE MATERIALS SCIENCE MANUFACTURER®
Now Invent.™
27 ANNIVERSARY

American Elements
Opens a World of Possibilities
...Now Invent!
www.americanelements.com

AIP Publishing

All-fiber supercontinuum absorption spectroscopy for mid-infrared gas sensing

Cite as: APL Photon. 9, 111303 (2024); doi: 10.1063/5.0230383
Submitted: 23 July 2024 • Accepted: 21 October 2024 •
Published Online: 12 November 2024

View Online Export Citation CrossMark

Rémi Bizot,[1] Idris Tiliouine,[2] Frédéric Désévédavy,[1,a)] Grégory Gadret,[1] Clément Strutynski,[1] Esteban Serrano,[1] Pierre Mathey,[1] Bertrand Kibler,[1] Sébastien Février,[2] and Frédéric Smektala[1]

AFFILIATIONS

[1] Laboratoire Interdisciplinaire Carnot de Bourgogne (ICB), UMR 6303 CNRS-Université Bourgogne Franche-Comté, Avenue Alain Savary, 21000 Dijon, France
[2] Institut de Recherche XLIM, UMR 7252 CNRS-Université de Limoges, 87000 Limoges, France

Note: This paper is part of the APL Photonics Special Topic on Mid-IR Photonics.
[a)] **Author to whom correspondence should be addressed:** frederic.desevedavy@u-bourgogne.fr

ABSTRACT

The development of compact fiber-based light sources emitting over a wide wavelength range in the mid-infrared and their application to the detection of greenhouse gases and volatile organic compounds still remain of critical interest. In the present work, we make use of several dedicated infrared fibers for implementing a mid-infrared optical device pumped by a thulium doped-fiber laser around 1.965 μm that simultaneously enables a first nonlinear stage of frequency conversion and supercontinuum generation and a second linear stage of gas absorption spectroscopy. As a proof-of-principle, we carry out mid-infrared supercontinuum absorption spectroscopy of methane around 7.7 μm by means of a hollow-core fiber-based gas cell combined to a commercial Fourier-transform infrared spectrometer. Our all-fiber configuration operating in the femtosecond regime at megahertz repetition rate allows the detection of methane concentrations as low as 20 ppm.

© 2024 Author(s). All article content, except where otherwise noted, is licensed under a Creative Commons Attribution (CC BY) license (https://creativecommons.org/licenses/by/4.0/). https://doi.org/10.1063/5.0230383

16 December 2024 13:28:14

I. INTRODUCTION

As the concentration of greenhouse gases in the atmosphere has increased since the industrial revolution, contributing significantly to global warming,[1] the monitoring and measurement of atmospheric pollutants is essential. Among the technological solutions for the detection of greenhouse gases, optical detection by means of spectroscopic measurements is attracting growing interest. For this reason, the mid-infrared (mid-IR) range is very attractive, as it corresponds to the molecular fingerprint region extending from 2 to 20 μm, which is the fundamental absorption range for chemical species.[2] Optical gas sensors based on thermal emitters suffer from low sensitivity due to their limited brightness in the infrared, making detection of low concentrations difficult.[3] Solutions based on the latest generation of low-noise sub-mW light-emitting diodes in the mid-IR have proved effective in detecting greenhouse gases with detection limits below the ppm level.[3] However, the narrow spectral bandwidth of this type of source means that multiple species cannot be detected simultaneously. The development of broadband infrared sources based on supercontinuum (SC) generation in optical fibers has therefore become a key area of research. SC sources can cover the visible to mid-IR range with high brightness, even outperforming synchrotron sources, and high coherence,[4–11] thus impacting many applications, including spectroscopy[10] and gas detection.[4,12–15] While fluoride and tellurite fibers enable SC generation up to 5 μm,[4,10,13,16,17] suitable glasses with broader mid-IR transparency are needed to cover the entire molecular fingerprint region of interest for spectroscopic detection.[5,8] The transparency window of chalcogenide glasses covers such a spectral range, in particular Se- and Te-based glasses. Thanks to their strong nonlinear optical properties, these glasses are also particularly suitable for generating SC far in the mid-IR.[2,18,19]

Here, we demonstrate the effectiveness of infrared fiber cascading (made of fluoride and chalcogenide glasses) as a frequency shifter and SC source for greenhouse gas supercontinuum absorption spectroscopy (SAS) in the mid-IR range by means of a gas cell made of

© Author(s) 2024

hollow-core fiber. As a proof-of-principle experiment, we detect the strong absorption band of methane (CH_4) located at the early beginning of the band III atmospheric window (at 7.7 μm) by means of our all-fiber device, far from the initial pumping laser in the 2-μm waveband.

II. EXPERIMENTAL SETUP

A. Chalcogenide glass and fiber fabrication

In the following, we briefly present the fabrication of chalcogenide glasses and the drawing of the step index optical fiber used for generating the mid-IR SC source. It is worth noting that the elements composing our As-free glasses match with the environmental requirements of the European REACH regulation.[20] The core and clad glass compositions are part of the Ge–Se–Te ternary system and are located in the Se-rich part of the pseudo-binary $GeSe_4$–$GeTe_4$ system that allows for stable glass preparation compatible with fiber drawing.[21] Cladding and core compositions are, respectively, $Ge_{20}Se_{70}Te_{10}$ and $Ge_{20}Se_{60}Te_{20}$. Glass rods are synthetized by the melt quenching method. Stoichiometric quantity of 5 N raw starting products as well as oxygen and hydrogen getters Al (5 N; 50 ppm wt.) and $TeCl_4$ (4.5 N; 1000 ppm wt.), respectively, are introduced in a silica ampoule, which is then evacuated down to secondary vacuum (10^{-5} mbar) during several hours before being sealed. After a first synthesis of 10 h at 850 °C in a rocking furnace that ends by a quenching in water followed by an annealing step around glass transition temperature (T_g), the obtained glass rod is inserted in a new silica ampoule to be further purified by means of two successive distillations. The first one occurs under dynamic vacuum (plugged to the vacuum pump). Volatile impurities are collected in the liquid nitrogen cooled trap of the vacuum pumping set up, while refractory particles stay in the starting batch. The glass condensates in the receiving batch. Next, the ampoule is sealed and a static distillation by means of a two-zone furnace is used to remove the last traces of refractory particles such as C, Al_2O_3, or SiO_2. Finally, the ampoule is sealed again and placed in a rocking furnace for 10 h at 850 °C before being quenched in water and annealed around T_g. The rod-in-tube method is then employed to prepare step-index preforms, which are then drawn to fiber with a controllable outer diameter between 100 and 400 μm providing a core size ranging between 5 and 20 μm.

B. All-fiber mid-IR SC generation

Recently, mid-IR femtosecond fiber laser sources based on soliton self-frequency shift have been reported to be efficient for producing high-peak power solitons between 3 and 4.5 μm.[22–25] Our fiber-based SC source consists of a cascade of optical fibers excited by means of a custom-designed laser emitting sub-ps μJ-pulses at 1.965 μm at the repetition rate of 1 MHz (see the experimental setup depicted in Fig. 1). Two custom-designed large mode area fibers first provide continuous Raman soliton self-frequency shift up to 3.1 μm. A third, commercially available, fluoroindate fiber shifts the radiation further up to 4.1 μm. Finally, the chalcogenide fiber, with a core diameter of 14 μm, described above is used for SC generation in the 3–8 μm spectral band. Soliton self-frequency shift stages result from a judicious selection in terms of dispersive and nonlinear features of silica and fluoride optical fibers and mode matching for fiber-to-fiber couplings as well (see the table of Fig. 1). More details can be found in Refs. 22–26. Briefly, we first exploit multi-soliton fission and soliton self-frequency shift in large mode-area silica and

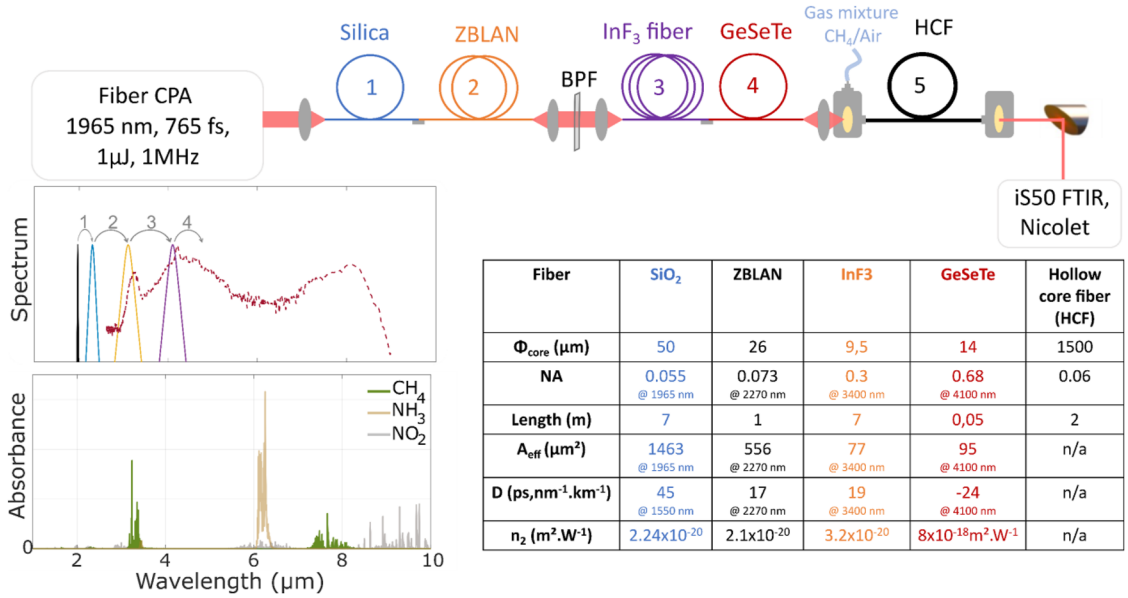

Fiber	SiO_2	ZBLAN	InF3	GeSeTe	Hollow core fiber (HCF)
Φ_{core} (µm)	50	26	9,5	14	1500
NA	0.055 @ 1965 nm	0.073 @ 2270 nm	0.3 @ 3400 nm	0.68 @ 4100 nm	0.06
Length (m)	7	1	7	0,05	2
A_{eff} (µm²)	1463 @ 1965 nm	556 @ 2270 nm	77 @ 3400 nm	95 @ 4100 nm	n/a
D (ps,nm^{-1}.km^{-1})	45 @ 1550 nm	17 @ 2270 nm	19 @ 3400 nm	-24 @ 4100 nm	n/a
n_2 (m².W^{-1})	2.24×10^{-20}	2.1×10^{-20}	3.2×10^{-20}	8×10^{-18} m².W^{-1}	n/a

FIG. 1. Top: All-fiber scheme of the experimental setup for mid-IR SC generation and SAS experiments (cascading of five fibers). Bottom left: Principle of operation of our four cascaded nonlinear stages of frequency conversion and SC generation in the mid-IR range, and the corresponding absorption bands of some greenhouse gases addressed by our fiber SC light source. Bottom right: Table listing the physical parameters of optical fibers used.

16 December 2024 13:28:14

© Author(s) 2024

ZBLAN fibers. A 500-nm bandpass filter (BPF) centered at 3 μm is then used to select the first ejected and redshifted 90-fs (500-kW) soliton, before the very last frequency-shifting stage occurring in the rather small-core InF_3 fiber. We then obtain a fiber-based source of highly energetic femtosecond pulses (8.5 nJ, 180 fs) at 4.1 μm. It is worth noting that the BPF is also used to filter out short wavelengths that might damage the Ge–Se–Te fiber. In addition, it isolates the soliton of interest to measure the power delivered at 4.1 μm by this cascaded pump source. Next, an additional nonlinear propagation stage is added by means of butt-coupling into a short segment (5-cm long) of the chalcogenide fiber above-described for SC generation over the 3–8 μm spectral band. The present all-fiber SC source is similar to Ref. 26, with one fluoride fiber stage less, which simplifies the whole fiber SC source. All fiber parameters listed in the table of Fig. 1 are given close to the input pulse wavelength coupled into each fiber segment. A similar, all fibered, mid-IR SC source has been demonstrated in Ref. 27. It is based on SC cascading, which requires cascading two chalcogenide fibers: one sulfide (which has dispersion and bandpass properties closer to fluoride) and one selenide to reach 10 μm. In contrast, the mid-IR source we developed utilizes only one chalcogenide fiber (a selenide) and delivers a signal up to 9 μm. The mid-IR SC source developed in this study is based on first generating a soliton redshift, which then pumps a nonlinear chalcogenide fiber, whereas the source in Ref. 27 relies on the redshift of an initial SC generated in a silica fiber pumped in the long-pulse regime (pulse width around 500 ps). This configuration is well-known to prevent any preservation of initial pulse coherence, unlike our present approach, as demonstrated in Sec. III. It is also worth noting that we did not fully optimize the setup for a broad spectrum; instead, we focused on optimizing the power in the 7–8 μm range to enable CH_4 spectroscopic measurements, as detailed in Sec. III.

C. Fiber-based gas cell

The generated SC is then coupled into the final stage of SAS by means of a ZnSe lens, namely the gas cell made of a commercially available multimode hollow-core fiber.[28] The latter consists of a plastic capillary whose inner surface is coated with a layer of stainless steel, onto which a layer of AgI is deposited, forming an IR reflective inner coating. Each extremity of the fiber is connected to a block equipped with a ZnSe optical window, a SMA connector, and a gas connection port. The fiber parameters are as follows: 2-m-long connectorized patchcord, 3–14 μm transmission window with 1 dB/m loss, 1.5-mm internal diameter, and 1 atm for maximum pressure. The output signal of the gas cell is sent to spectral characterization provided by a commercial Fourier-transform infrared (FTIR) spectrometer by means of a gold-coated parabolic mirror. The choice of a hollow-core fiber is driven by the easy input and output light couplings together with a sufficient light–gas interaction length for sensing applications when compared to multi-pass cells.[3,15,29–32] For gas control, two gas cylinders are required: the analyte gas cylinder (CH_4, 2250 ppm) and a dry air one (80%N_2, 20%O_2) for carrying out dilutions. Two flowmeters allow the adjustment of the gas concentration in the hollow-core fiber. We emphasize that a fairly long time (a few minutes) is respected to ensure the homogeneity of the mixture into the gas cell. Figure 1 (bottom left) also shows the principle of operation of our all-fiber supercontinuum absorption spectroscopy for mid-IR gas sensing, thus highlighting the interest of the cascaded fiber approach as an alternative to other bulky laser chains. A compact architecture for spectral shifting and subsequent broadening of fiber laser pulses into the mid-IR allows us to cover the molecular fingerprint region of greenhouse gases, in particular here for methane spectroscopy.

It is worth noting that although some free-space optical components or free-space couplings remain, there already exist some solutions for their integration into fiber devices. Regarding the bandpass filter (BPF), it can indeed be integrated into the fiber by inscribing a Bragg grating, which has already been demonstrated in fluoride fibers.[33] The coupling between silica and fluoride fibers can be achieved through mechanical butt-coupling or splicing.[34,35] As this work is a proof of principle, we did not prioritize the removal of free-space optical components.

III. RESULTS

Figure 2(a) shows both cladding and core glass losses measured on single-index fibers drawn from the corresponding glass rods together with a cross section view of the obtained step-index fiber fabricated by employing the rod-in-tube method. Despite similar purification processes, the attenuation background level (about 3–5 dB/m) is higher than in our previous work,[23] in particular for the cladding glass. We attribute these wavelength-independent losses to remaining extrinsic scattering centers that were not eliminated during the distillation steps. Indeed, the conditions (heating rate, vacuum level, and temperature gradient) under which distillations are performed can be responsible for impurities such as Al_2O_3, SiO_2, or C to being entrained into the distilled glass.[36,37] However, since a very short fiber segment (5 cm long) is required for mid-IR SC generation in the femtosecond pumping regime,[19,21] the present loss level is negligible. A 14-μm core step-index Ge–Se–Te fiber was chosen as the best compromise between nonlinear and dispersive features, and efficient light coupling as well. The selected fiber did not lead to the broadest SC but rather to the highest power spectral density at the target wavelength of 7.7 μm. The spectral dependence of the core and cladding refractive indices was approximated by Sellmeier's law described in Ref. 21. Then, the parameters of the fundamental mode (effective area and group velocity dispersion) were calculated by solving the dispersion equation (also called the eigenvalue equation) for cylindrical step-index fibers for the core diameter of 14 μm. The calculated dispersion curve of the fundamental guided mode is shown in Fig. 2(b), whereas the nonlinear coefficient at 4.1 μm was found to be 0.14 W^{-1} m^{-1}. Our fiber exhibits a zero-dispersion wavelength (ZDW) around 5.9 μm so that it provides a normal dispersion at the input soliton pulse wavelength. Such dispersive features might produce SC with a reduced spectral bandwidth but better coherence properties[23,38] even if soliton dynamics will take place during spectral broadening beyond the ZDW. The experimental spectra of input soliton pulse and generated mid-IR SC are depicted in Fig. 2(c). The residual signal at 3 μm comes from the second stage of soliton shift in the ZBLAN fiber. The SC bandwidth measured at −20 dB extends from 2.8 to 8.2 μm (70 THz bandwidth). We clearly observed a symmetric spectral broadening around the pumping wavelength due to self-phase modulation, which then extends beyond the ZDW with a solitonic shape centered around 7.65 μm. A longer propagation distance into

16 December 2024 13:28:14

© Author(s) 2024

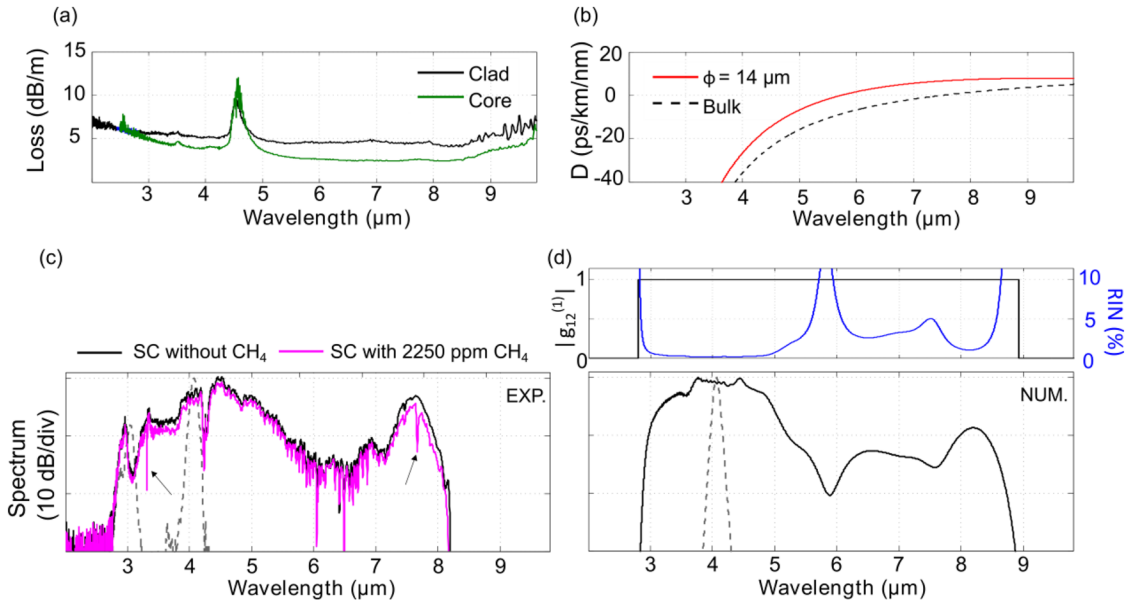

FIG. 2. (a) Attenuation curves of single-index fibers made of clad and core glasses. (b) Calculated chromatic dispersion of our step-index Ge–Se–Te fiber together with the material bulk dispersion. (c) Experimental SC spectrum (black solid line) generated in the 5-cm-long step-index Ge–Se–Te fiber pumped at 4.1 μm with soliton pulse (black dashed line). SAS measurement for a CH_4 content of 2250 ppm (magenta line). Arrows indicate the two mid-IR absorption bands of methane around 3.3 and 7.7 μm. (d) Corresponding numerical simulation of SC generation (bottom: averaged SC and pump spectra; top: SC coherence and RIN profiles).

the fiber shows a soliton self-frequency shift up to 8.5–9.0 μm (see the illustration in Fig. 1); however, we here keep this shorter segment for SAS as delivering a higher signal-to-noise ratio around 7–8 μm (i.e., our spectral range of interest). This behavior is corroborated by our numerical simulations based on the generalized nonlinear Schrödinger equation taking into account fiber parameters and the measured pump pulse features [see Fig. 2(d)]. Additional numerical characterization of the SC stability is provided through the calculation of modulus of the complex degree of first-order coherence $g_{12}^{(1)}$ and relative intensity noise (RIN) with an ensemble average of 50 simulations,[38,39] by taking into account the quantum noise only (in the form of one-photon-per-mode noise). We then reveal that the spectral coherence almost appears insensitive to quantum noise mainly due to the dispersion regime, but the RIN profile clearly depends on the dispersion sign: it is very low in the normal dispersion regime, but then increases and exceeds the % level in the anomalous dispersion regime with soliton dynamics. This level of RIN is still compatible with SAS at the sub-ppm level. Note that including an additional technical noise contribution, related to the stability of the pump pulses (i.e. amplitude noise), would affect both frequency-dependent profiles of coherence and RIN.[39]

Our all-fiber SC configuration at 1-MHz repetition rate enables a satisfactory average output power reaching 3 mW, which allows us to use a 2-m-long hollow-core fiber as a gas cell. The subsequent SC light collected at the output of the hollow-core fiber covers the 3–8 μm range within a dynamic range of 20 dB; the remaining total average power is above 1 mW. Our SC bandwidth and good enough signal-to-noise ratio are usable for methane spectroscopy at its fundamental absorption band that lies between 7.3 and 7.88 μm. The magenta curve in Fig. 2(c) shows the SC in the presence of CH_4 flow only. Methane absorption lines are clearly visible around 3.3 and 7.7 μm (see arrows). One can also note CO_2 absorption around 4.26 μm already present in the free-space optical path to the FTIR spectrometer. Regarding the two absorption peaks observed in the 6–6.5 μm, according to the HITRAN database, there are no CH_4 absorption bands with intensities comparable to those at 3.3 μm or 7.7 μm. However, strong water absorption bands are present, which explains why the signal intensity and the signal-to-noise ratio are lower in this region. Thus, those absorptions peaks are likely measurement artifacts caused by variations in humidity in the room atmosphere between the reference scan (pure dry air) and the sample scan (2500 ppm of CH_4). Our setup is sensitive to these humidity variations due to the free space between the hollow fiber output and the FTIR. In the following, we vary the CH_4 concentration to determine the sensitivity of the device. First, typical SC stability was characterized through the measurement of successive SC spectra with a dry air-filled gas cell; an example of calculated zero-absorbance line between two spectra is shown in Fig. 3(a). The uncertainty for absorbance and transmittance is, respectively, ±3% across the examined spectral range, which can be directly related to the RIN sensitivity to technical noise above described. Next, to control the variation in methane gas concentration, the flow rate was adjusted in relation to that of synthetic air. Variable flows were prescribed, representing concentrations of 173, 135, 90, 45, and 22 ppm. Figure 3(b) shows the different absorption/transmission curves for various CH_4 concentrations and the corresponding theoretical curves from the HITRAN database.[40] We notice a fairly good agreement between experimental measurements and theoret-

16 December 2024 13:28:14

© Author(s) 2024

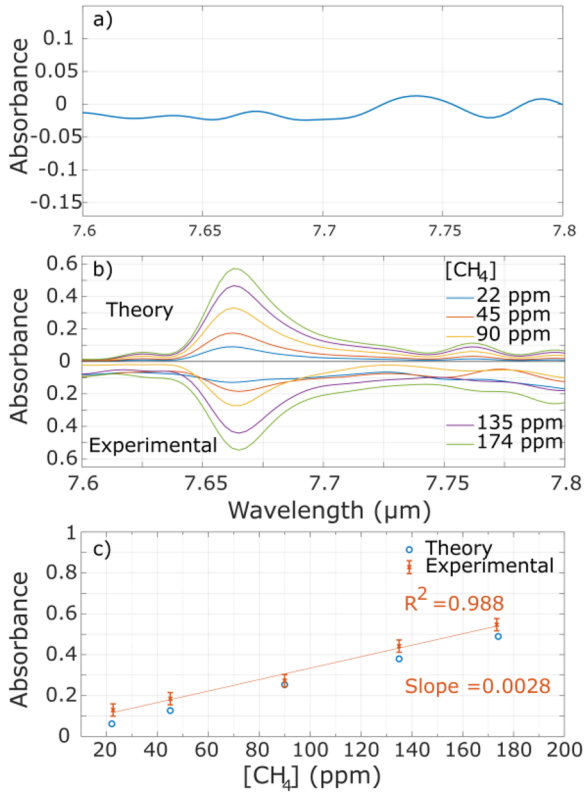

FIG. 3. (a) Zero absorbance spectrum calculated from two successive measurements of SC spectrum. (b) Theoretical and experimental methane absorptions, in the 7.6–7.8 μm range, obtained with our gas cell for various concentrations. (c) Corresponding absorbance values at 7.68 μm for increasing methane concentration and corresponding linear fit.

ical calculations of absorbance. A linear operation regime of the sensing device is also confirmed in Fig. 3(c). SAS for CH_4 sensing at 1.68 μm has been previously demonstrated with SC generated in silica fiber and by means of 2.4 m hollow core photonic bandgap fiber.[41] Although the absorption band of CH_4 at 1.68 μm is much weaker than that at 7.68 μm, the authors of Ref. 41 achieved a detection limit as low as 4 ppm for CH_4 sensing at 1.68 μm. This remarkable result was made possible through extensive optimization of both the SC source and the detection process, including SC noise reduction and integration time. In the present case, CH_4 sensing is performed at 7.68 μm, where the CH_4 absorption is significantly stronger, but the detection efficiency is lower due to the reduced sensitivity of mid-IR detectors. Furthermore, the stability of the SC source we have developed, based on cascaded fibers, is not comparable to that of Ref. 41, which employs a single silica fiber. In addition, we are operating with 1 mW average power for gas sensing, while the SC source described in Ref. 41 delivers ~9 mW measured after the gas cell. However, the minimum concentration that can be detected with our device is 22 ppm, i.e., a much better sensitivity than that previously presented with a similar device but using the absorption line around 3.3 μm[32] with a lower detection limit of 3×10^4 ppm. As the atmospheric concentration of methane is of the order of 1.9 ppm, the detection of variations of anthropogenic origin will require significant improvements to the system. We believe that reducing the technical noise of pumping sources and increasing the mid-IR SC average power will significantly enhance sensitivity and reduce the lower concentration threshold detection limit.

IV. CONCLUSION

In this study, we demonstrate the development of an all-fiber mid-infrared supercontinuum source covering the 3–8 μm spectral range in the femtosecond regime by means of cascading fiber architecture pumped by a thulium doped-fiber laser. Our compact SC source operating at 1-MHz repetition rate is then combined to a 2-m-long fiber-based gas cell to assess possible spectroscopic application, in particular by detecting methane at a wavelength of 7.68 μm, at low concentrations down to 22 ppm. The present results of our all-fibered supercontinuum absorption spectroscopy configuration are encouraging for the detection of gas mixtures, but also highlight some of the limitations of such supercontinuum sources related to pulse-to-pulse fluctuations. Future studies will have to address simultaneously both power scaling and noise issues of fiber supercontinuum sources to reach higher sensitivities.

ACKNOWLEDGMENTS

This work was supported by the French National Center for Scientific Research (CNRS) through a Ph.D. thesis grant. We thank the company *Le Verre Fluoré*, France, for the fabrication of the large mode area fluoride fiber.

This work was also supported by Agence Nationale de la Recherche (ISITE-BFC, Contract No. ANR-15-IDEX-03; EIPHI Graduate School, Contract No. ANR-17-EURE-0002; and EquipEx+ Smartlight, Contract Nos. ANR-21-ESRE-0040 and ANR-21-CE24-0001 MIRthFUL); Région Bourgogne Franche-Comté; and Conseil Régional de Nouvelle-Aquitaine (Grant No. Femto-VO2, MIR-X).

AUTHOR DECLARATIONS

Conflict of Interest

The authors have no conflicts to disclose.

Author Contributions

R.B. and I.T. contributed equally to this work.

Rémi Bizot: Investigation (equal); Methodology (equal). **Idris Tiliouine**: Conceptualization (equal); Investigation (equal); Methodology (equal). **Frédéric Désévédavy**: Conceptualization (equal); Investigation (equal); Methodology (equal); Visualization (equal); Writing – original draft (equal). **Grégory Gadret**: Methodology (equal). **Clément Strutynski**: Visualization (equal). **Esteban Serrano**: Investigation (equal); Software (equal). **Pierre Mathey**: Visualization (equal). **Bertrand Kibler**: Conceptualization (equal); Formal analysis (equal); Software (equal); Supervision (equal); Validation (equal); Writing – review & editing (equal). **Sébastien Février**: Conceptualization (equal); Investigation (equal); Supervision (equal); Validation (equal). **Frédéric Smektala**:

16 December 2024 13:28:14

© Author(s) 2024

Funding-acquisition (equal); Project-administration (equal); Resources (equal); Supervision (equal).

DATA AVAILABILITY

The data that support the findings of this study are available from the corresponding author upon reasonable request.

REFERENCES

[1]F. M. O Connor, O. Boucher, N. Gedney, C. D. Jones, G. A. Folberth, R. Coppell, P. Friedlingstein, W. J. Collins, J. Chappellaz, J. Ridley, and C. E. Johnson, "Possible role of wetlands, permafrost, and methane hydrates in the methane cycle under future climate change: A review," Rev. Geophys. **48**(4), RG4005 (2010).

[2]Z. Zhao, B. Wu, X. Wang, Z. Pan, Z. Liu, P. Zhang, X. Shen, Q. Nie, S. Dai, and R. Wang, "Mid-infrared supercontinuum covering 2.0–16 μm in a low-loss telluride single-mode fiber," Laser Photonics Rev. **11**(2), 1700005 (2017).

[3]N. Li, L. Tao, H. Yi, C. S. Kim, M. Kim, C. L. Canedy, C. D. Merritt, W. W. Bewley, I. Vurgaftman, J. R. Meyer, and M. A. Zondlo, "Methane detection using an interband-cascade led coupled to a hollow-core fiber," Opt. Express **29**(5), 7221–7231 (2021).

[4]I. Zorin, P. Gattinger, A. Ebner, and M. Brandstetter, "Advances in mid-infrared spectroscopy enabled by supercontinuum laser sources," Opt. Express **30**(4), 5222–5254 (2022).

[5]S. Dai, Y. Wang, X. Peng, P. Zhang, X. Wang, and Y. Xu, "A review of mid-infrared supercontinuum generation in chalcogenide glass fibers," Appl. Sci. **8**(5), 707 (2018).

[6]P. Froidevaux, A. Lemière, B. Kibler, F. Désévédavy, P. Mathey, G. Gadret, J.-C. Jules, K. Nagasaka, T. Suzuki, Y. Ohishi, and F. Smektala, "Dispersion-engineered step-index tellurite fibers for mid-infrared coherent supercontinuum generation from 1.5 to 4.5 μm with sub-nanojoule femtosecond pump pulses," Appl. Sci. **8**(10), 1875 (2018).

[7]Y. Leventoux, G. Granger, Y. Arosa, I. Tilouine, K. Krupa, A. Tonello, V. Couderc, and S. Février, "Three octave visible to mid-infrared supercontinuum generation seeded by multimode silica fiber pumped at 1064 nm," Opt. Lett. **48**(17), 4582 (2023).

[8]T. Sylvestre, E. Genier, A. N. Ghosh, P. Bowen, G. Genty, J. Troles, A. Mussot, A. C. Peacock, M. Klimczak, A. M. Heidt *et al.*, "Recent advances in supercontinuum generation in specialty optical fibers [invited]," J. Opt. Soc. Am. B **38**(12), F90–F103 (2021).

[9]J. M. Dudley and J. R. Taylor, *Supercontinuum Generation in Optical Fibers* (Cambridge University Press, 2010).

[10]F. Borondics, M. Jossent, C. Sandt, L. Lavoute, D. Gaponov, A. Hideur, P. Dumas, and S. Février, "Supercontinuum-based Fourier transform infrared spectromicroscopy," Optica **5**(4), 378 (2018).

[11]C. R. Petersen, P. M. Moselund, L. Huot, L. Hooper, and O. Bang, "Towards a table-top synchrotron based on supercontinuum generation," Infrared Phys. Technol. **91**, 182–186 (2018).

[12]B. Napier, O. Bang, C. Markos, P. Moselund, L. Huot, F. Harren, A. Khodabakhsh, H. Martin, F. O. Briano, L. Balet *et al.*, "Ultra-broadband infrared gas sensor for pollution detection: The TRIAGE project," J. Phys.: Photonics **3**, 031003 (2021).

[13]J. Kilgus, K. Duswald, G. Langer, and M. Brandstetter, "Mid-infrared stand-off spectroscopy using a supercontinuum laser with compact Fabry-Pérot filter spectrometers," Appl. Spectrosc. **72**(4), 634–642 (2018).

[14]K. Eslami Jahromi, M. Nematollahi, Q. Pan, M. A. Abbas, S. M. Cristescu, F. J. M. Harren, and A. Khodabakhsh, "Sensitive multi-species trace gas sensor based on a high repetition rate mid-infrared supercontinuum source," Opt. Express **28**(18), 26091 (2020).

[15]M. Abbas, K. Jahromi, M. Nematollahi, R. Krebbers, N. Liu, G. Woyessa, O. Bang, L. Huot, F. Harren, and A. Khodabakhsh, "Fourier transform spectrometer based on high-repetition-rate mid-infrared supercontinuum sources for trace gas detection," Opt. Express **29**(14), 22315–22330 (2021).

[16]S. Kedenburg, C. Strutynski, B. Kibler, P. Froidevaux, F. Désévédavy, G. Gadret, J.-C. Jules, T. Steinle, F. Mörz, A. Steinmann *et al.*, "High repetition rate mid-infrared supercontinuum generation from 13 to 53 μm in robust step-index tellurite fibers," J. Opt. Soc. Am. B **34**(3), 601–607 (2017).

[17]F. Désévédavy, C. Strutynski, A. Lemière, P. Mathey, G. Gadret, J.-C. Jules, B. Kibler, and F. Smektala, "Review of tellurite glasses purification issues for mid-IR optical fiber applications," J. Am. Ceram. Soc. **103**(8), 4017–4034 (2020).

[18]C. R. Petersen, U. Møller, I. Kubat, B. Zhou, S. Dupont, J. Ramsay, T. Benson, S. Sujecki, N. Abdel-Moneim, Z. Tang *et al.*, "Mid-infrared supercontinuum covering the 1.4–13.3 μm molecular fingerprint region using ultra-high NA chalcogenide step-index fibre," Nat. Photonics **8**(11), 830 (2014).

[19]A. Lemière, R. Bizot, F. Désévédavy, G. Gadret, J.-C. Jules, P. Mathey, C. Aquilina, P. Béjot, F. Billard, O. Faucher, B. Kibler, and F. Smektala, "1.7–18 µm mid-infrared supercontinuum generation in a dispersion-engineered step-index chalcogenide fiber," Results Phys. **26**, 104397 (2021).

[20]See https://echa.europa.eu/fr/regulations/reach/legislation for more information about the European REACH regulation for dangerous chemical substances limitations and risks management.

[21]A. Lemière, F. Désévédavy, P. Mathey, P. Froidevaux, G. Gadret, J.-C. Jules, C. Aquilina, B. Kibler, P. Béjot, F. Billard *et al.*, "Mid-infrared supercontinuum generation from 2 to 14 μm in arsenic- and antimony-free chalcogenide glass fibers," J. Opt. Soc. Am. B **36**(2), A183–A192 (2019).

[22]I. Tiliouine, H. Delahaye, G. Granger, Y. Leventoux, C. E. Jimenez, V. Couderc, and S. Février, "Fiber-based source of 500 kW mid-infrared solitons," Opt. Lett. **46**(23), 5890 (2021).

[23]B. Kibler, E. Serrano, A. Maldonado, L.-R. Robichaud, S. Duval, M. Bernier, R. Bizot, F. Désévédavy, R. Vallée, Y. Messaddeq, and F. Smektala, "All-fiber 2-6 μm coherent supercontinuum source based on chalcogenide fibers pumped by an amplified mid-IR soliton laser," Opt. Commun. **542**, 129568 (2023).

[24]S. Duval, J.-C. Gauthier, L.-R. Robichaud, P. Paradis, M. Olivier, V. Fortin, M. Bernier, M. Piché, and R. Vallée, "Watt-level fiber-based femtosecond laser source tunable from 28 to 36 μm," Opt. Lett. **41**(22), 5294–5297 (2016).

[25]H. Delahaye, G. Granger, J.-T. Gomes, L. Lavoute, D. Gaponov, N. Ducros, and S. Février, "Generation of 35 kW peak power 80 fs pulses at 29 μm from a fully fusion-spliced fiber laser," Opt. Lett. **44**(9), 2318–2321 (2019).

[26]I. Tiliouine, G. Granger, C. Jimenez-Durango, Y. Leventoux, B. Wetzel, V. Couderc, and S. Février, "Two-octave spanning supercontinuum from a 4.53 µm fiber-based laser," Results Phys. **47**, 106326 (2023).

[27]G. Woyessa, K. Kwarkye, M. K. Dasa, C. R. Petersen, R. Sidharthan, S. Chen, S. Yoo, and O. Bang, "Power stable 1.5–10.5 µm cascaded mid-infrared supercontinuum laser without thulium amplifier," Opt. Lett. **46**(5), 1129–1132 (2021).

[28]See https://guidingphotonics.com/ for more details about the mid IR hollow core fibers used as gas cell.

[29]D. Francis, J. Hodgkinson, B. Livingstone, P. Black, and R. P. Tatam, "Low-volume, fast response-time hollow silica waveguide gas cells for mid-IR spectroscopy," Appl. Opt. **55**(25), 6797 (2016).

[30]M. Nikodem, G. Gomólka, M. Klimczak, D. Pysz, and R. Buczynski, "Demonstration of mid-infrared gas sensing using an anti-resonant hollow core fiber and a quantum cascade laser," Opt. Express **27**(25), 36350 (2019).

[31]P. Patimisco, A. Sampaolo, L. Mihai, M. Giglio, J. Kriesel, D. Sporea, G. Scamarcio, F. Tittel, and V. Spagnolo, "Low-loss coupling of quantum cascade lasers into hollow-core waveguides with single-mode output in the 3.7–7.6 μm spectral range," Sensors **16**(4), 533 (2016).

[32]A. Lemière, A. Maldonado, F. Désévédavy, B. Kibler, P. Mathey, G. Gadret, J.-C. Jules, N. P. T. Hoa, T. Suzuki, Y. Ohishi, and F. Smektala, "Towards absorption spectroscopy by means of mid-infrared supercontinuum generation in a step index tellurite fiber," Laser Phys. **31**(2), 025702 (2021).

[33]A. Fuerbach, G. Bharathan, and M. Ams, "Grating inscription into fluoride fibers: A review," IEEE Photonics J. **11**(5), 1–11 (2019).

[34]R. A. Martinez, G. Plant, K. Guo, B. Janiszewski, M. J. Freeman, R. L. Maynard, M. N. Islam, F. L. Terry, O. Alvarez, F. Chenard, R. Bedford, R. Gibson, and

16 December 2024 13:28:14

© Author(s) 2024

A. I. Ifarraguerri, "Mid-infrared supercontinuum generation from 16 to >11 μm using concatenated step-index fluoride and chalcogenide fibers," Opt. Lett. **43**(2), 296–299 (2018).
[35]K. Guo, R. A. Martinez, G. Plant, L. Maksymiuk, B. Janiszewski, M. J. Freeman, R. L. Maynard, M. N. Islam, F. L. Terry, R. Bedford *et al.*, "Generation of near-diffraction-limited, high-power supercontinuum from 157 μm to 12 μm with cascaded fluoride and chalcogenide fibers," Appl. Opt. **57**(10), 2519–2532 (2018).
[36]V. Shiryaev, S. Mishinov, and M. Churbanov, "Investigation of adhesion of chalcogenide glasses to silica glass," J. Non-Cryst. Solids **408**, 71–75 (2015).
[37]J. S. Sanghera, L. E. Busse, and I. D. Aggarwal, "Effect of scattering centers on the optical loss of As_2S_3 glass fibers in the infrared," J. Appl. Phys. **75**(10), 4885–4891 (1994).
[38]G. Genty, S. Coen, and J. M. Dudley, "Fiber supercontinuum sources (Invited)," J. Opt. Soc. Am. B **24**(8), 1771–1785 (2007).
[39]E. Genier, P. Bowen, T. Sylvestre, J. M. Dudley, P. Moselund, and O. Bang, "Amplitude noise and coherence degradation of femtosecond supercontinuum generation in all-normal-dispersion fibers," J. Opt. Soc. Am. B **36**(2), A161 (2019).
[40]See https://hitran.org/ database for spectroscopic parameters of CH_4.
[41]A. I. Adamu, M. K. Dasa, O. Bang, and C. Markos, "Multispecies continuous gas detection with supercontinuum laser at telecommunication wavelength," IEEE Sens. J. **20**, 10591 (2020).

16 December 2024 13:28:14

© Author(s) 2024